(113) (116) (Scan kell) arXiv-ba 2000 Varsó COSPAR

C2.4-0015 COSPAR WARSAW 2000

SPATIAL AND TEMPORAL VARIATION OF ACOUSTIC GRAVITY WAVES AND SUDDEN IMPULSE-LIKE NEUTRAL DENSITY CHANGES IN THE THERMOSPHERE

E. Illés - Almár[1], P. Bencze[2], I. Almár[1]

[1]*Konkoly Observatory, H- 1525 Budapest, P.O.B. 67, Hungary*
[2]*Geodetic and Geophysical Research Institute, H-9401 Sopron, P.O.B.5, Hungary*

ABSTRACT

The Italian San Marco V satellite was orbiting above the Equator in the height range of 130 - 600 km in 1988. Using measurements of its DBI accelerometer several kinds of wave-like variation of the total density have been studied already in earlier papers. The present paper gives account of the discovery of four kinds of wave-like phenomena of short characteristic time scale: 1/ sudden neutral density decreases, 2/ sudden impulse-like increases of the total density, 3/ certain AGWs that supposed to be connected with spatial resonance, 4/ sudden increases in the amplitude of the AGWs at certain heights. An attempt is made to find some explanation of their characteristics and their origin.

Introduction

This paper is a part of a series of publications in which the authors deal with changes of the total neutral density on a small spatial and temporal scale (Illés-Almár et al., 1997, 1998a, 1998b, Almár et al., 1999, Bencze et al., 1999). These investigations were made possible by the high time resolution of the total neutral density measurements on board of the San Marco V satellite (Arduini et al., 1992, 1993). The data of the accelerometric measurements revealed not only atmospheric acoustic and gravity waves in the thermosphere, but also processes related to gravity waves, e.g. the effect of plasma instabilities, spatial resonance like variations and sudden, impulse like changes, indicating that the interaction of the ionized and the neutral component of the atmosphere is in action not only in case of large dimensions, but also in volumes of smaller extension.

Data

The total density values derived from the measurements of the DBI microaccelerometer on board of the Italian San Marco V satellite follow each other every second in average. The inclination of the orbit of the satellite was 3°, thus it enabled the investigation of the phenomena in the neighborhood of the equator. The data base refers to the height interval 130 - 600 km and to the time interval between April and December 1988 (this was a period of rising solar activity and of weak geomagnetic activity). The majority of the measurements were carried out above 250 km, lower heights have been reached by orbital decay only in the last ten days. In Figure 1 the change of the height range is plotted as a function of time. It is obvious that seasonal variations can not be studied in detail on this material.

Description of the Phenomena

Trying to improve some upper-atmospheric models we came to the conclusion that residuals $f = \rho^{measured}/\rho^{model}$ present a scatter considerably larger than it should be on the basis of the accuracy of the measurements. Using CACTUS microaccelerometer data and statistical methods by Illés-Almár et al., (1996) this scatter has been interpreted as a consequence of the effect of atmospheric density waves, then investigated on the San Marco V material of higher temporal resolution as case studies (Illés-Almár et al., 1998b, Almár et al., 1999). Based on such investigations we have discovered four different phenomena with short characteristic time scale in the neutral upper atmosphere: 1/ sudden neutral density depletions (NDD); 2/ sudden, impulse-like neutral density increases or giant "solitary" wave-like variations (GW); 3/ spatial resonance like fluctuations; 4/ a sudden increase with height in the amplitude of atmospheric waves (SAI).

Sudden Neutral Density Depletions (NDD): The NDDs are sudden decreases in the total density with a characteristic time of several 10 sec and with amplitudes of 10 - 20%. Some examples are given in Figure 2. Altogether 248 such cases have been identified (Illés-Almár et al., 1998a, 1998b, Bencze et al., 1999). The NDDs occur sometimes alone, sometimes within a series. Altogether 149 of the 248 NDDs belong to series, the longest one contains 11 NDDs.

Giant Wave-like Variations (GW): GWs are sudden density increases or giant waves with amplitudes of 10 - 90% of the total density, exceeding 7 - 10 times the amplitudes of the surrounding waves. Altogether 53 such cases have been found. Figure 3 shows some examples of GWs.

Spatial Resonance: We have found only one clear example (Figure 4) of such kind of variation. On 26.08.1988 (MJD 47399) at 18,26 - 19,83 hours LST the satellite orbiting in the altitude range of 383 to 332 km and a longitude range of 166 - 188^{o} crossed a region where the amplitude of the atmospheric waves was much larger than in the surrounding i.e. before and after this region. In this case the resonance character can clearly be seen.

Sudden Amplitude Increases of Atmospheric Waves (SAI): According to the accelerometric measurements there are always waves in the upper-atmosphere and their amplitude is increasing with height (Illés-Almár et al., 1996, 1997, 1998b, Almár et al., 1999). The rate of the increase, however, is not continuous but it changes suddenly at certain altitude (380 - 450 km) which depends on local time. Above this altitude-level the wave amplitude is always large, but never under this turning point. The only exception is the above mentioned spatial resonance-like variation. In Figure 5 there are some examples for SAIs.

Results of Statistical Investigations

If the study of the nature and origin of these phenomena is the task to be fulfilled, then first the temporal and spatial occurrence of the phenomena must be cleared. Thus, for NDDs and GWs the diurnal (Figure 6) and the longitudinal variation (Figure 7) while for NDDs, GWs and for the starting points of SAIs the height variation (Figure 8) of the occurrence frequency of the phenomena have been investigated. As it can be seen in Figure 6 , the *diurnal variation* of the occurrence of the two phenomena indicates maximum values at night. It is to be noted that in the case of the GWs the small number of the cases is a disturbing problem.

In Figure 7 the *longitudinal distribution* of the occurrence frequency has a maximum between 30 - 60^{o} for NDDs and between 150 - 240^{o} for GWs. The dominant feature of the longitudinal variation of the occurrence frequency of GWs is a broad maximum. This region corresponds to the area of the Pacific Ocean, which circumstance may be interesting from the point of view of the interpretation of the data.

In Figure 8 the *height distributions* of the occurrence frequency of the NDDs, GWs as well as that of the starting points of the SAIs are demonstrated. The height distribution of NDDs shows a sharp maximum at 250 km (with better resolution see also Figure 9), while that of GWs indicates a height distribution extending to a broad height range from 150 km to 550 km. The height distribution of the occurrence of the starting points of SAIs is limited to the height range from 350 to 500 km. There was never an increased amplitude of the waves at lower altitudes, but always at higher altitudes. The height of the change of the amplitude depends on LST (Figure 10).

Discussion

<u>Neutral Density Depletions (NDD)</u>

The results in connection with the NDDs are and will be published in (Illés-Almár et al., 1998a, 1998b, Bencze et al., 1999). Here we summarize them very briefly. The NDDs are dominantly night phenomena. They start to appear after 17 hour LST, and maximize at 18-20 and 0-4 hours (Figure 6). Figure 9 shows the height distribution with 20 km resolution. The maximum occurs at 250 km, at the bottom of the F layer. In longitude the maximum occurs at 30-60 degrees (Figure 7). Our view is that their origin can be in connection with the well-known plasma bubbles. The rising plasma bubbles, namely, can carry the neutral component of the atmosphere via ion drag, causing density decreases. Model calculation and a case study strengthen this hypothesis (Bencze et al., 1999).

Giant Wave-like Variations (GW)

This phenomenon might be due to shock waves of magnetospheric origin propagating in the thermosphere, or due to interference of waves originating from both auroral ovals. In both cases the equatorial orbit is the most suitable to study the sudden impulse-like increases.

Concerning the GWs, the *diurnal variation* of this phenomenon (Figure 6) hints at a mostly night-time process producing these impulse-like solitary waves. As it can be seen, the height distribution (Figure 8) of these waves indicates two maxima, one in the height region of the F layer "valley" (150-200 km), where the electron density is smaller between the E and F regions of the night-time ionosphere, and the other in the night-time F region of the ionosphere. Thus, both observations might support the assumption that the GWs are mostly due to a night-time process.

A possible source for the double nighttime maxima (see Figure 6) of GWs might be the substorm (*Baistörung*) phenomenon. Substorms discovered in the changes of the geomagnetic field in the premidnight and postmidnight hours are related to processes in the tail of the magnetosphere, to the sudden release of energy accumulated in the tail. The energy input into the auroral zone is accompanied by an intensification of the current flowing in the auroral oval and thus a sudden heating (Joule heating) of the neutral upper atmosphere. As a result of this heating, an impulse like expansion of the atmosphere takes place along the active part of the auroral oval. The intensification of the current [DP1 current system (Clauer and McPherron, 1974; Clauer and Kamide, 1985)] and thus, the increased heating along the active part of the auroral oval can be observed before midnight (~22^h)and after midnight (~02^h). Considering the temporal occurrence of the neutral density impulse propagating equatorwards to the vicinity of the equator, one must take into account a time lag of the disturbance. Assuming a 2 hours time delay, the impulse-like disturbances may appear after 24^h and 04^h, respectively. The disturbances arriving from the northern and southern hemisphere can amplify each other leading to the formation of an impulse of large amplitude. However, further investigations are needed for the proof of this suggestion.

The maximum appearing at 18 - 20 hours in the diurnal variation might be related to the sudden change of the direction of the electric field in the F region from eastward to westward due to the prereversal enhancement of the eastward electric field (Heelis et al., 1974). This sudden change of the electric field would mean a sudden switch over from a gravitationally stable condition of the plasma to for the moment gravitationally unstable conditions. This process may be indicated by the neutral density too. At sunrise, on the contrary, the change from the westward to the eastward electric field is already gradual.

In connection with the *height distribution* (Figure 8) of GWs it is to be noted that irregularities appear in the F region valley on geomagnetically moderately disturbed nights (Shen et al., 1976). The impulse like disturbances indicated in the height distribution of these changes between 150 and 200 km might be related to the irregularities in the F layer valley activity, where gravity waves are generated. This circumstance might be connected with the occurrence of GWs in the F region valley, too.

As regards the *longitudinal variation* (Figure 7) of the occurrence of GWs, a definite maximum appears in the longitude region from 150° to 270°, coinciding with the equatorial zone of the Pacific Ocean, a zone of strong convection.

Spatial Resonance

The orbit of the San Marco V satellite was especially suitable for the study of the assumed spatial resonance, since spatial resonance for thermospherically launched gravity waves can occur only near the equator (Beer, 1973). There is no such restriction for spatial resonance created by gravity waves of tropospheric origin, but in this case the phenomenon can not appear at heights above 300 km. It can be mentioned in advance that this height of occurrence of the resonance effect corresponds to the height range of the night-time F region of the ionosphere.

As it is known, spatial resonance occurs if the drift of ionospheric irregularities due to an electric field has the same velocity as the phase velocity of an internal atmospheric gravity wave (Whitehead, 1971). The drift motion of these ionospheric irregularities depends on the extension of the electric field and on the orientation of the irregularities as compared to the geomagnetic field. The spatial resonance mechanism causes the resonant amplification of the irregularities and also that of the neutral density variations. The spatial resonance criteria can be written in the following form (Beer, 1973)

$$U = V_o \qquad \text{or} \qquad \Omega = k \cdot V_o = k_z \mu_H E_{ox} \tag{1}$$

$$k_z = \left[\frac{\mathrm{Im}(K_z)\mu_H |E_{ox}| - \beta}{D_x \cos^2\Theta + D_y \sin^2\Theta} \right]^{1/2} \quad \text{that is} \quad \frac{\gamma g}{2c^2}\cos\Theta \mu_H |E_{ox}| > \beta \qquad (2)$$

where U is the phase velocity of the internal gravity wave, Ω is the angular frequency of the gravity wave, k is the real part of the complex wave number, V_o stands for the velocity of charged particle (drift velocity). Furthermore, k_z and Im (K_z) are the real and imaginary parts of the complex wave number, respectively, μ_H represents the Hall mobility, $|E_{ox}|$ is the absolute value of the horizontal component of the electric field, β is the recombination coefficient, D_x , D_y are the diffusion coefficients referring to diffusion to magnetic east and parallel to the magnetic field, respectively, Θ is the dip angle, while γ is the ratio of specific heats, g acceleration due to gravity and c the speed of sound.

As it is known, the energy transported by internal gravity waves is propagating from its source upwards, the phase velocity of the gravity waves is oriented downwards. Thus, regarding Eq. (1), the inequality $\Omega / k_z < U_z < 0$ must be valid, consequently E_{ox} is also less than zero, indicating that spatial resonance can only be produced in case of westward electric fields. The drift measurements carried out in Jicamarca (11.95 S, 283.14 E), show that the electric field is westward in the F region by night from cca. 19^h to 6^h in the morning (Woodman, 1970; Fejer et al., 1979). Thus, according to the first spatial resonance criterion the resonance phenomenon observed in the data of the San Marco V satellite might be due to spatial resonance. The fulfillment of the second criterion can be controlled by substituting appropriate values into Eq. (2). As a result of the substitution it has been found that the inequality is fulfilled, if $\Theta \sim 0$; that is in the vicinity of the dip equator. As the measurement of the total neutral density were carried out in the neighborhood of the dip equator, the second criterion confirms also the assumption that the resonant phenomenon found in the data might be attributed to spatial resonance. This is in agreement with the establishment that the spatial resonance mechanism can only be effective near the equator in case of gravity waves generated in the thermosphere. However, according to theoretical considerations, tropospheric gravity waves can also generate spatial resonance at the base of the night-time F region at low and mid-latitudes (Beer, 1973). As it is known, first of all the equatorial area of the Pacific Ocean is the location of strong convective activity, thus, it is also an intense source of gravity waves.

Sudden Amplitude Increases of Atmospheric Waves (SAI)

Figure 10 shows the height and the density versus LST diagram for the onset of the amplitude increase of the atmospheric waves. It can be seen, that the amplitudes start to increase at higher altitudes at daytime than at night. The measured density versus LST plot demonstrates, however, that this switch-on appears generally at the same density value, that is in the h(LST) diagram only the effect of the diurnal bulge is visible.

Concerning this amplitude increase phenomenon, its explanation might be related to the special conditions in the height range above 300 km, where it can be observed. Gravity waves arriving from below can be recorded in the thermosphere. These waves are generated in the troposphere or in the thermosphere itself. The analyses of the waves indicated that they are incoherent, superposed oscillations. However, this circumstance alone would not enable the observation of the SAI phenomenon. Forced oscillations can only be of transient nature, if the conditions are stable from the point of view of dynamics of the atmosphere. In the thermosphere the temperature increases with increasing altitude and approaches the exospheric temperature. Thus, above a given height the atmosphere can be considered as isotherm. This means the change of the dynamical equilibrium from a stable state to at least indifferent state, eventually to an unstable state. Instability can develop and resonance phenomenon might occur due to convective instability. This mechanism is independent of the period below the Brunt-Vaisala frequency. In such a situation only a very small energy is needed for the increase of the amplitude, because of the small density of the atmosphere in this height region. On the basis of this hypothesis both the temporal and the spatial variations of this "resonance" phenomenon found in course of the analysis of the data might be explained, if the corresponding variations of atmospheric gravity wave activity is taken into account. This investigation will be the topic of another paper.

Acknowledgment

The authors are indebted to C. Arduini and to G. Laneve for the San Marco V material, to G. Laneve and to J. Nuspl for helpful discussions, to Mrs. M. Nagy for the computer work and to Mr. P. Decsy for the preparation of the manuscript.

References

Almár, I., Illés-Almár, E., Bencze, P., Laneve, G. (1999): Investigation of the variation of the neutral density wave pattern on the basis of San Marco V data. Adv. Space Res., **24** (11), 1605-1608.

Arduini, C., Broglio, L., Ponzi, U., Laneve, G. (1992): S.Marco V wavelike phenomena detected by the DBI instrument, Paper C.5-M.3.11, XXIX COSPAR, Washington D.C.

Arduini, C., Broglio, L., Ponzi, U. (1993): DB measurements in the San Marco D/L mission, Adv. Space Res. **13**, 185

Beer, T. (1973): Spatial resonance in the ionosphere. Planet Space Sci., **21**., 297-307.

Bencze, P., Almár, I., Illés-Almár, E. (1999): Further results referring to the neutral density depletions attributed to plasma bubbles, accepted for publication JASTP, paper no. MR 1505

Clauer, C. R., Mc Pherron, R. L. (1974): Mapping the local time - universal time development of magnetospheric substorms using mid-latitude magnetic observations. J. Geophys. Res., **79,** 2811-2820.

Clauer, C. R., Kamide, Y. (1985): DP1 and DP2 current systems for the March 22, 1979 substorms. J. Geophys. Res., **90**, 1343-1354.

Fejer, B. G., Farley, D. T., Woodman, R. F., Calderon, C. (1979): Dependence of equatorial F-region vertical drifts on season and solar cycle. J. Geophys. Res., **84,** 5792-5796.

Heelis, R. A., Kendall, P. C., Moffett, R. J., Windle, D. W., Rishbeth, H. (1974): Electrical coupling of the E and F regions and its effect on F-region drifts and winds. Planet. Space Sci., **22**, 743-756.

Illés-Almár, E., Almár I., Bencze P. (1996): Observational results hinting at the coupling of the thermosphere with the ionosphere/magnetosphere system and with the middle atmosphere, Adv. Space Res. **18** (3) 45-48

Illés-Almár E., Almár I., Bencze P. (1997): Investigation of the density wave activity in the thermosphere above 220 km, Adv. Space Res. **20** pp. 1273-1276

Illés-Almár, E., Almár, I., Bencze, P. (1998a): Neutral density depletions attributed to plasma bubbles. J. Geophys. Res., **103,** 4115-4116.

Illés-Almár, E., Almár, I., Bencze, P., Laneve, G. (1998b): Wave-like variations and sudden density decreases in the lower thermosphere as measured by the San Maro V satellite, accepted for publication in Physics and Chemistry of the Earth.

Shen, J. S., Swartz, W. E., Farley, D.T., Harper, R. M. (1976): Ionization layers in the nighttime E region valley above Arecibo. J. Geophys. Res., **81,** 5517-5526.

Whitehead, J. D. (1971): Ionization disturbances caused by gravity waves in he presence of an electrostatic field and background wind. J. Geophys. Res, **76,** 238-241.

Woodman, R. F. (1970): Vertical drift velocities and east-west electric fields at the magnetic equator. J. Geophys. Res., **75**, 6249-6259.

Figure Captions

Fig. 1. Altitude of the San Marco V satellite as a function of time.

Fig. 2. Examples of neutral density depletion (NDD) at different times and in different heights.

Fig. 3. Examples of the impulse-like changes (GW) at different times and in different heights.

Fig. 4. A spatial resonance phenomenon in the total neutral density.

Fig. 5. Examples of the wave amplitude increase (SAI) in the total neutral density at different times and in different heights.

Fig. 6. Diurnal variations of the occurrence of neutral density depletions (NDDs at the top), and that of the impulse-like changes of the neutral density (GWs below).

Fig. 7. Longitudinal variations of the occurrence of the neutral density depletions (NDDs at the top), and that of the impulse-like changes of the neutral density (GWs below).

Fig. 8. Height distribution of the occurrence of the neutral density depletions (NDDs at the top), that of the impulse-like changes of the neutral density (GWs in the middle) and that of the sudden amplitude increase phenomenon (SAIs below).

Fig. 9. Height distribution of the occurrence of the neutral density depletions (NDDs) with 20 km resolution.

Fig. 10. Diurnal variations of the height (at the top) and of the measured density (below) for the sudden amplitude increase (SAI) phenomenon.

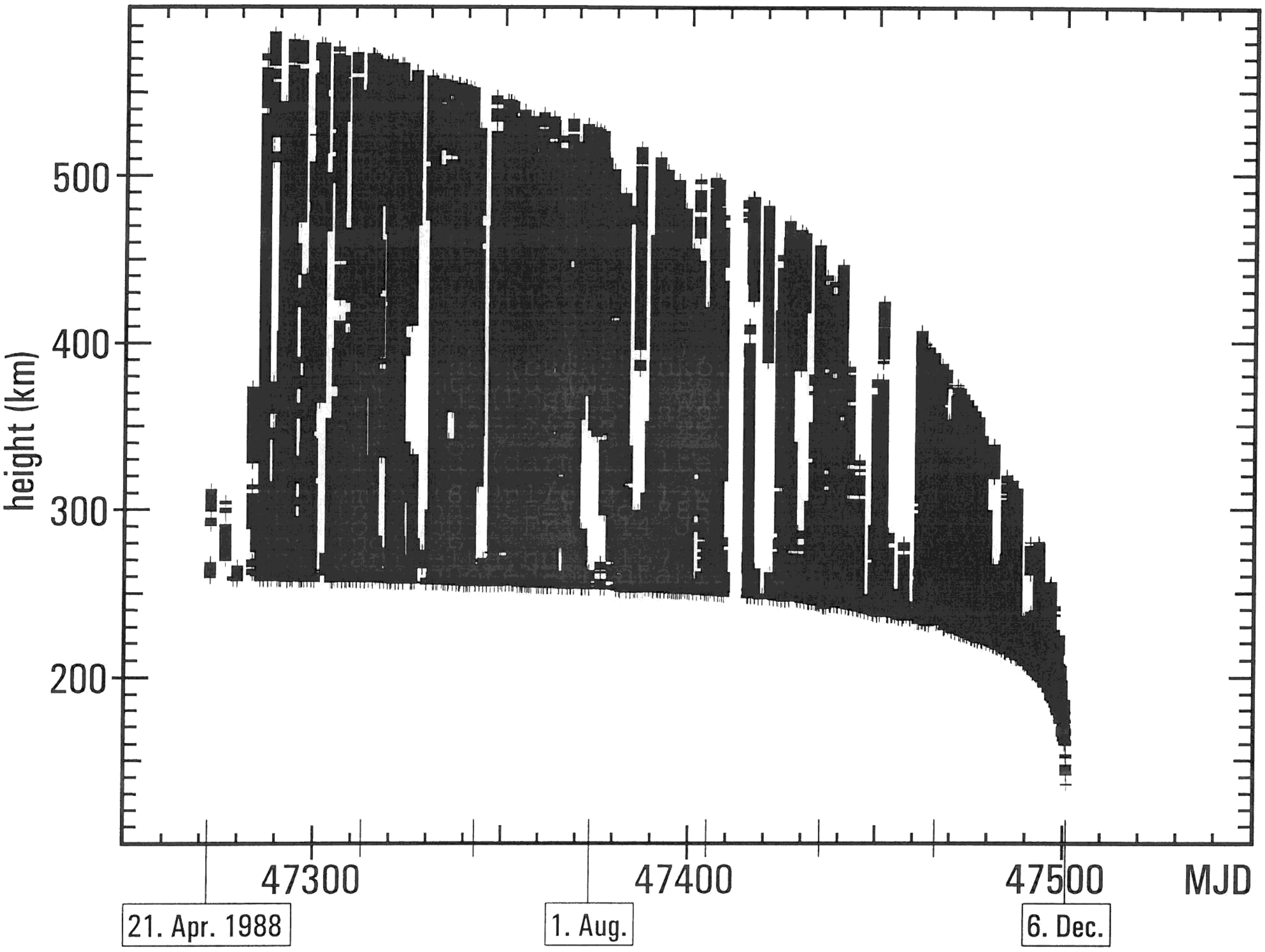

500
400
300
200
height (km)
47300
47400
47500
MJD
21. Apr. 1988
1. Aug.
6. Dec.

Fig. 1

véplepes 2001 jún Fig2ke.doc

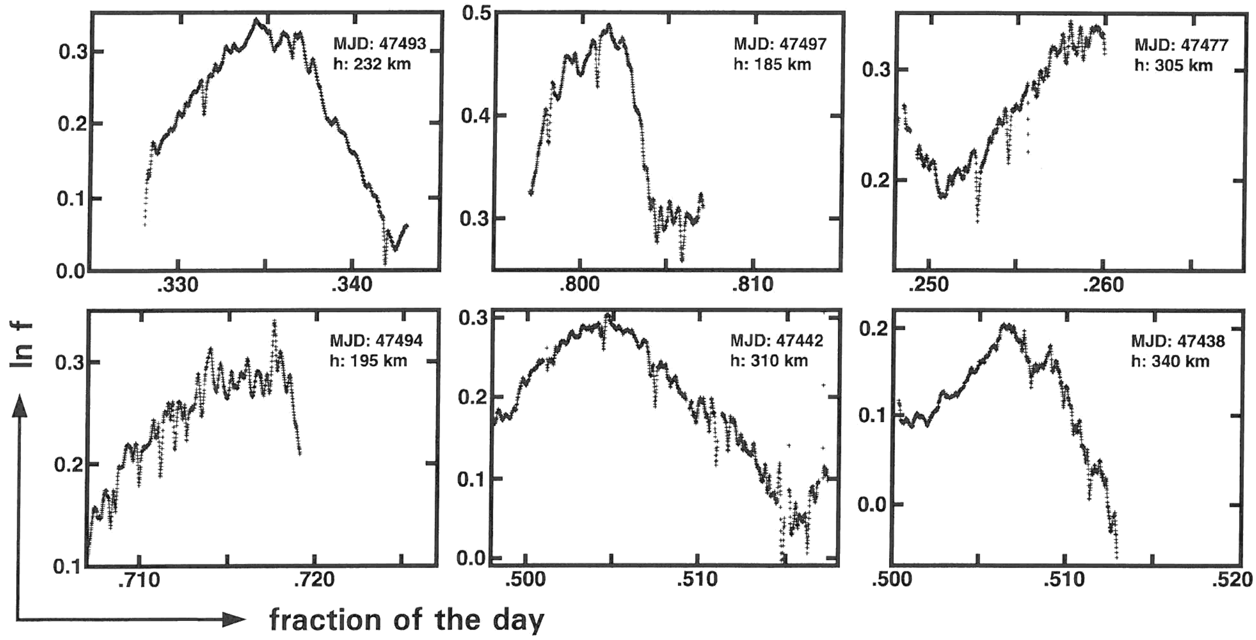

Fig. 2

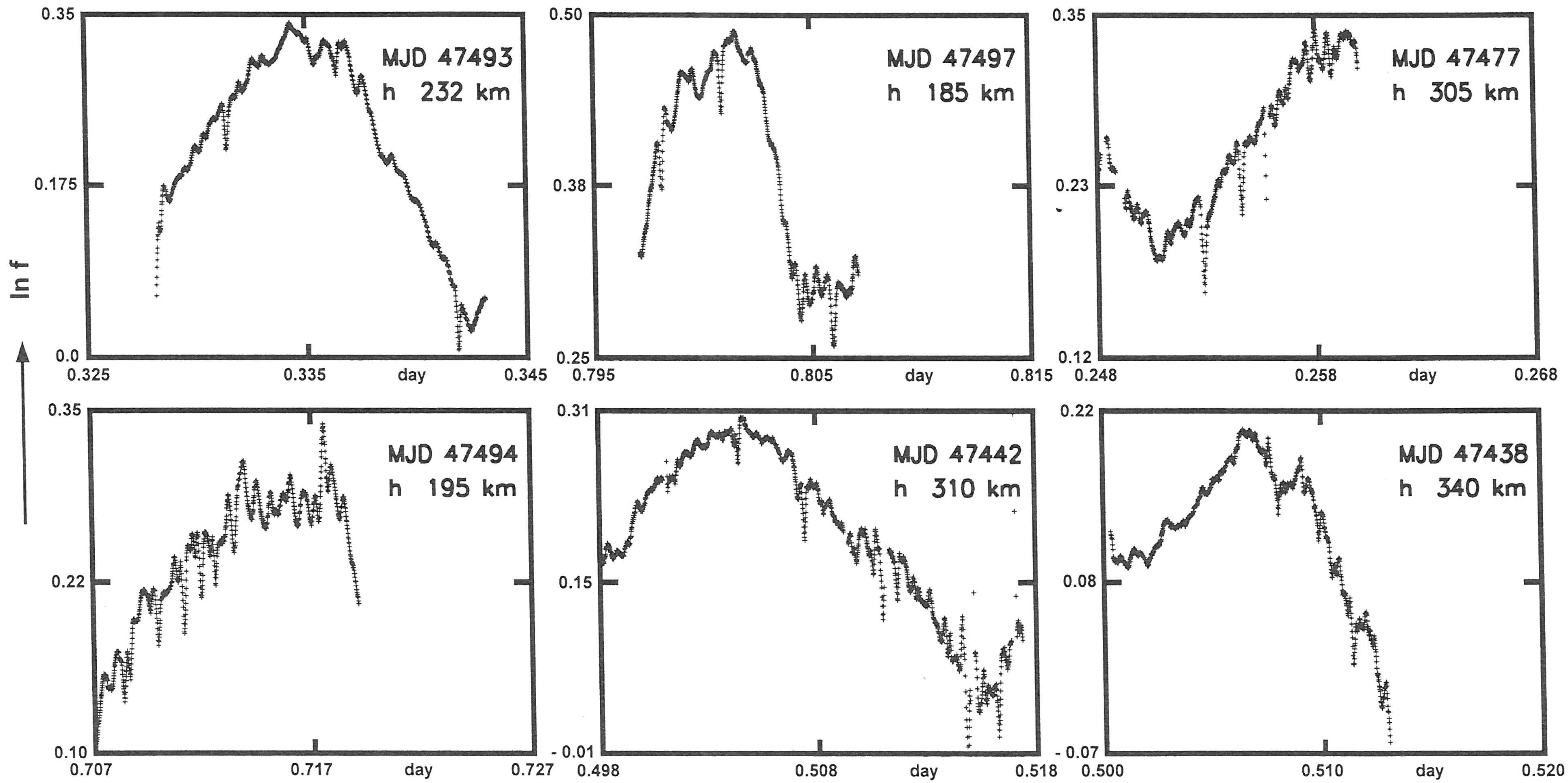
ln f
MJD 47493
h 232 km
0.35
0.175
0.0
0.325
0.335
day
0.345
MJD 47497
h 185 km
0.50
0.38
0.25
0.795
0.805
day
0.815
MJD 47477
h 305 km
0.35
0.23
0.12
0.248
0.258
day
0.268
MJD 47494
h 195 km
0.35
0.22
0.10
0.707
0.717
day
0.727
MJD 47442
h 310 km
0.31
0.15
- 0.01
0.498
0.508
day
0.518
MJD 47438
h 340 km
0.22
0.08
- 0.07
0.500
0.510
day
0.520

Fig. 2

vdplaspes 2001 jou Fig3ke.doc

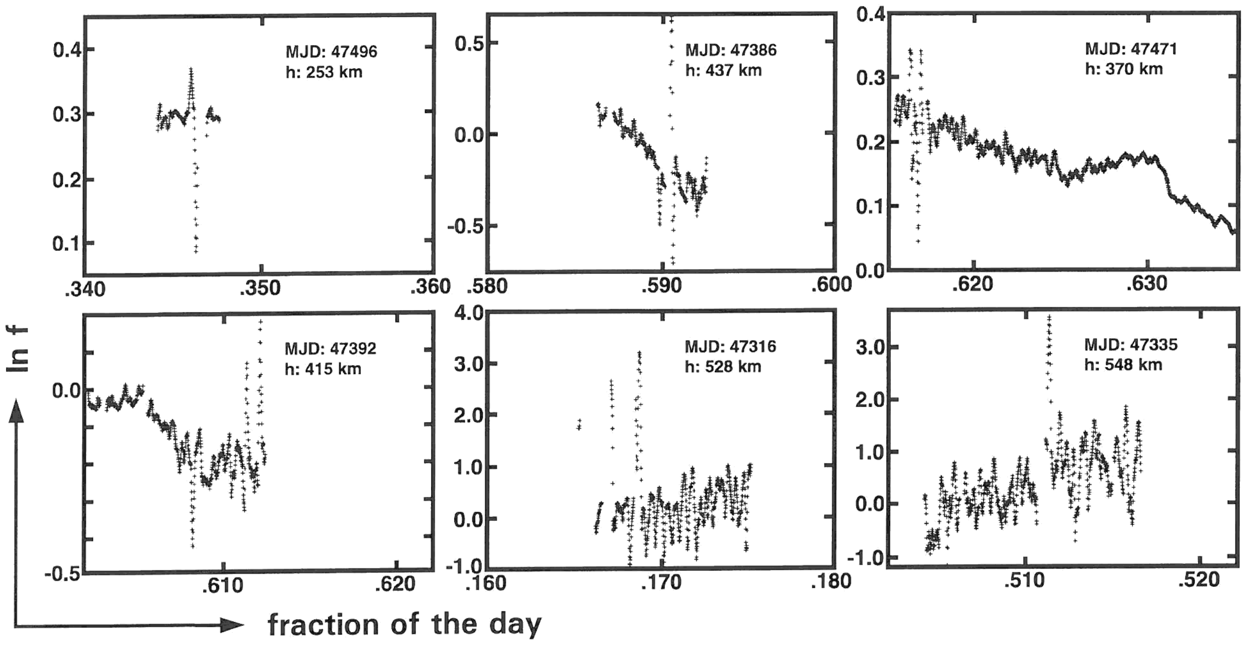

Fig. 3

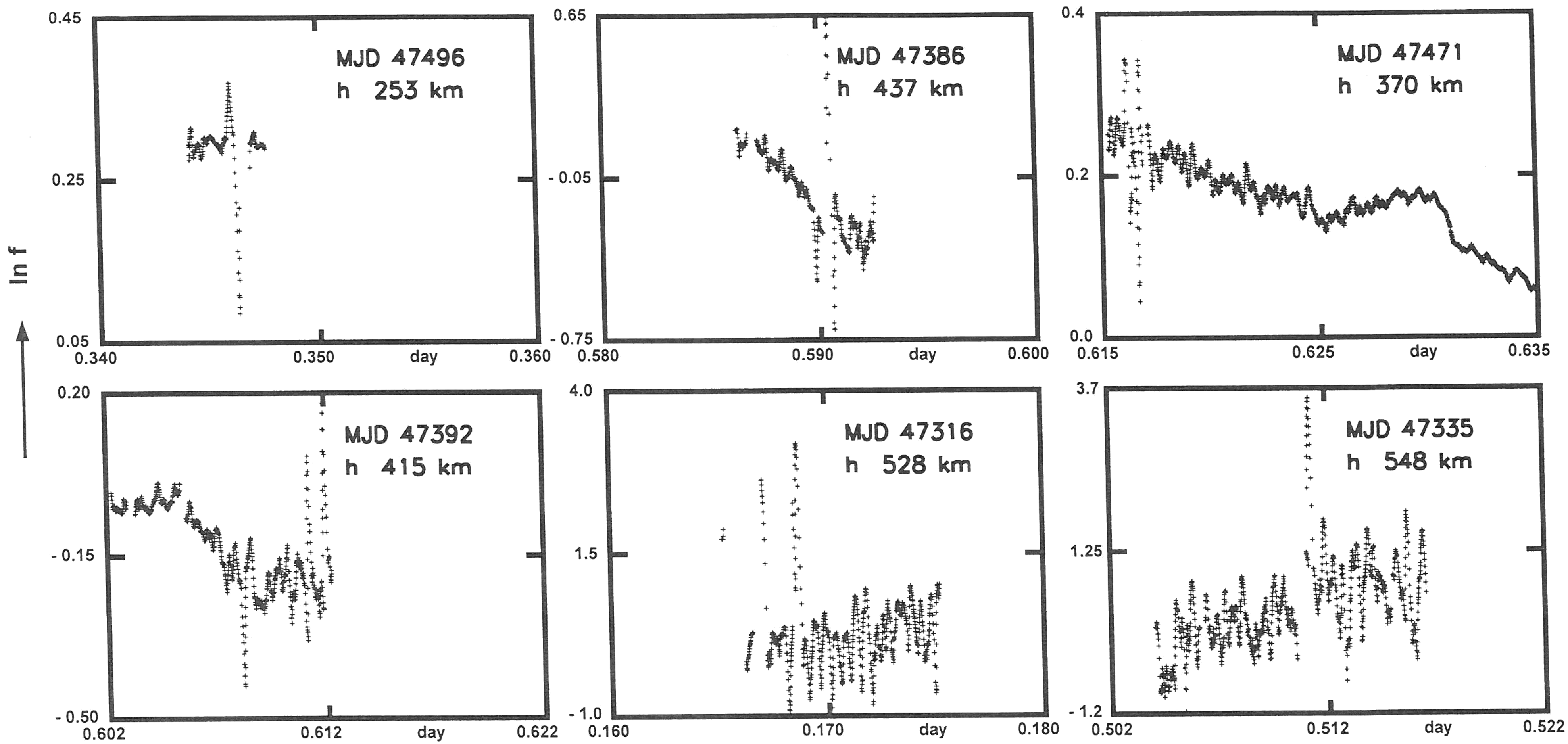
ln f
0.45
0.25
0.05
0.340
0.350
day
0.360
MJD 47496
h 253 km
0.65
- 0.05
- 0.75
0.580
0.590
day
0.600
MJD 47386
h 437 km
0.4
0.2
0.0
0.615
0.625
day
0.635
MJD 47471
h 370 km
0.20
- 0.15
- 0.50
0.602
0.612
day
0.622
MJD 47392
h 415 km
4.0
1.5
- 1.0
0.160
0.170
day
0.180
MJD 47316
h 528 km
3.7
1.25
- 1.2
0.502
0.512
day
0.522
MJD 47335
h 548 km

Fig. 3

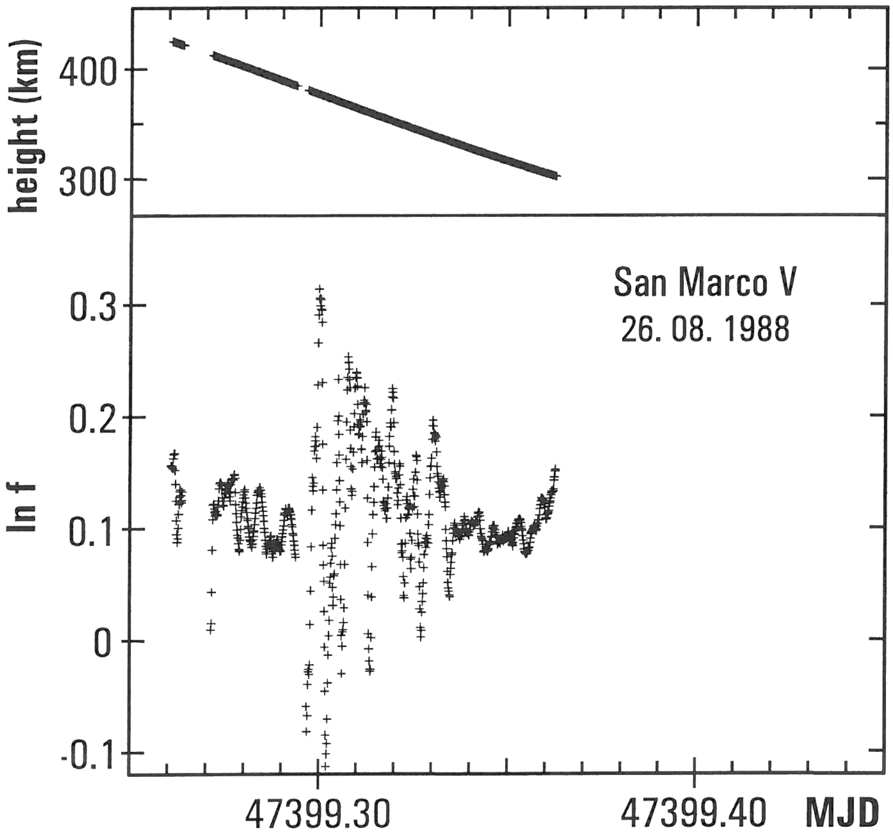
height (km)
400
300
San Marco V
26. 08. 1988
ln f
0.3
0.2
0.1
0
-0.1
47399.30
47399.40
MJD

Fig. 4

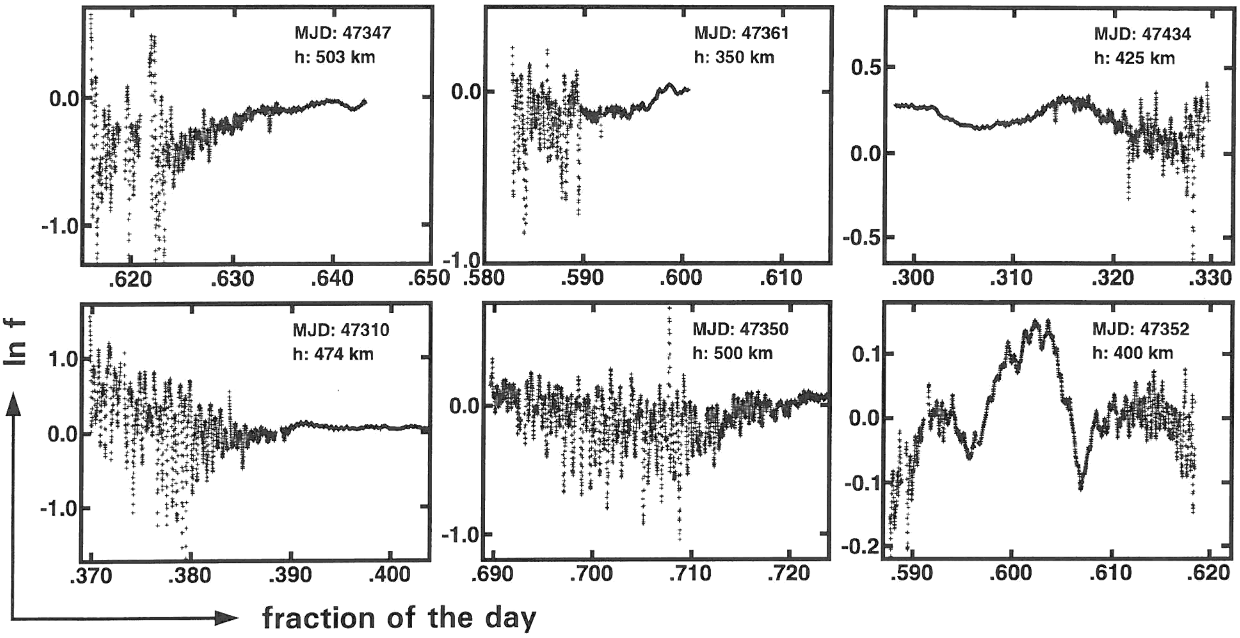
MJD: 47347
h: 503 km
MJD: 47361
h: 350 km
MJD: 47434
h: 425 km
MJD: 47310
h: 474 km
MJD: 47350
h: 500 km
MJD: 47352
h: 400 km
ln f
fraction of the day

Fig. 5

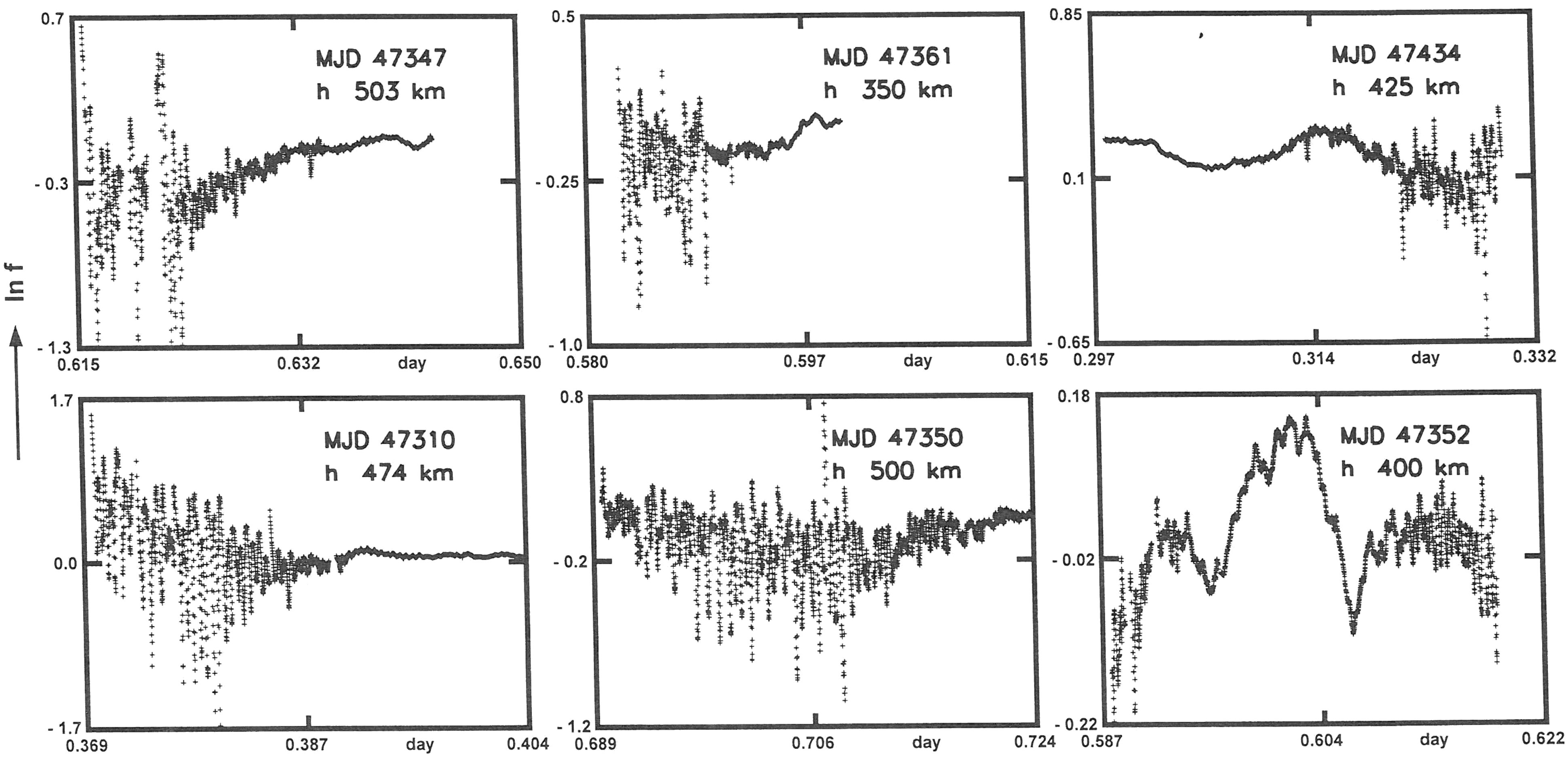
ln f
MJD 47347
h 503 km
0.7
- 0.3
- 1.3
0.615
0.632
day
0.650
MJD 47361
h 350 km
0.5
- 0.25
- 1.0
0.580
0.597
day
0.615
MJD 47434
h 425 km
0.85
0.1
- 0.65
0.297
0.314
day
0.332
MJD 47310
h 474 km
1.7
0.0
- 1.7
0.369
0.387
day
0.404
MJD 47350
h 500 km
0.8
- 0.2
- 1.2
0.689
0.706
day
0.724
MJD 47352
h 400 km
0.18
- 0.02
- 0.22
0.587
0.604
day
0.622

Fig. 5

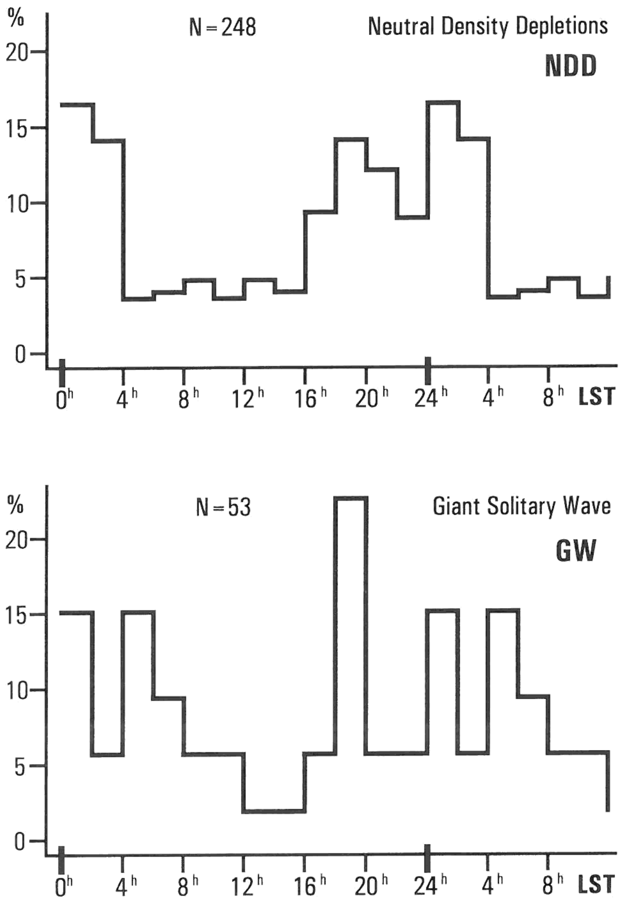
%
20
15
10
5
0
N = 248
Neutral Density Depletions
NDD
0h 4h 8h 12h 16h 20h 24h 4h 8h LST
%
20
15
10
5
0
N = 53
Giant Solitary Wave
GW
0h 4h 8h 12h 16h 20h 24h 4h 8h LST

Fig. 6

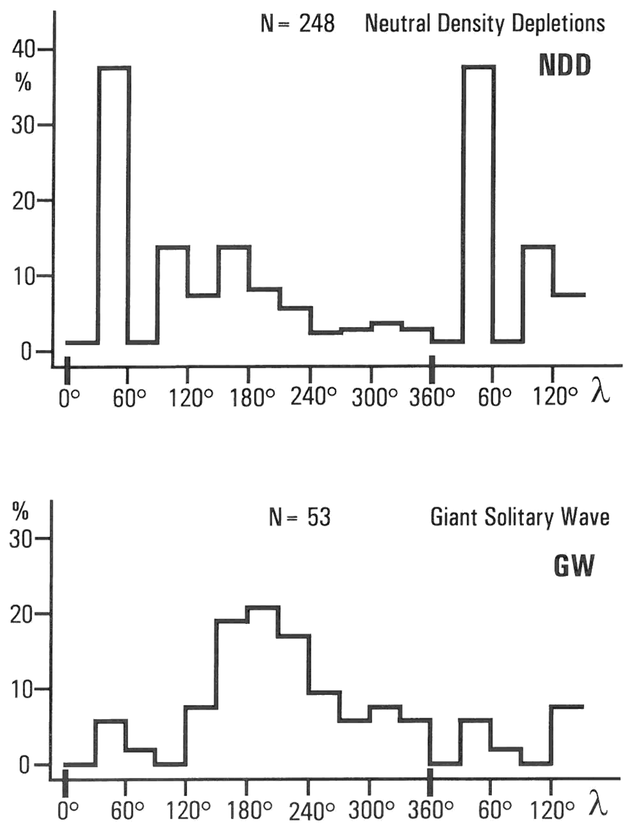
N = 248 Neutral Density Depletions
NDD
40
%
30
20
10
0
0° 60° 120° 180° 240° 300° 360° 60° 120° λ
%
30
N = 53 Giant Solitary Wave
GW
20
10
0
0° 60° 120° 180° 240° 300° 360° 60° 120° λ

Fig. 7

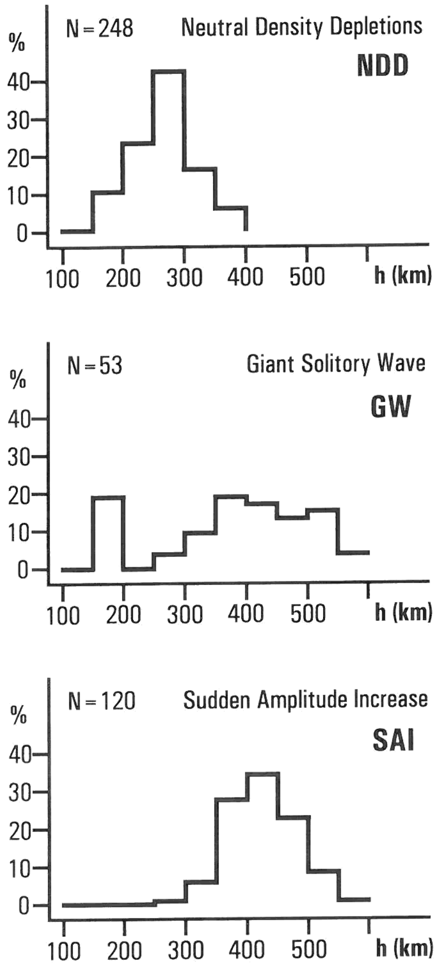
N = 248
Neutral Density Depletions
NDD
%
40
30
20
10
0
100
200
300
400
500
h (km)
N = 53
Giant Solitory Wave
GW
%
40
30
20
10
0
100
200
300
400
500
h (km)
N = 120
Sudden Amplitude Increase
SAI
%
40
30
20
10
0
100
200
300
400
500
h (km)

Fig. 8

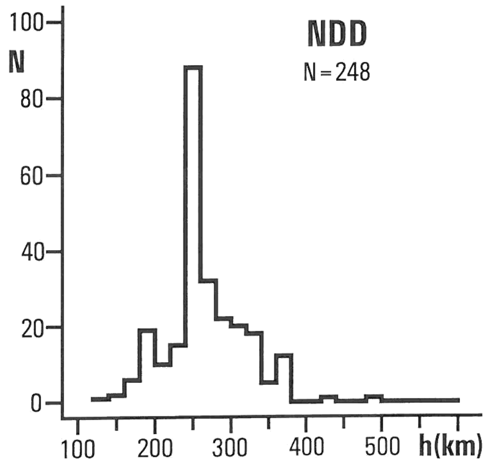

Fig. 9

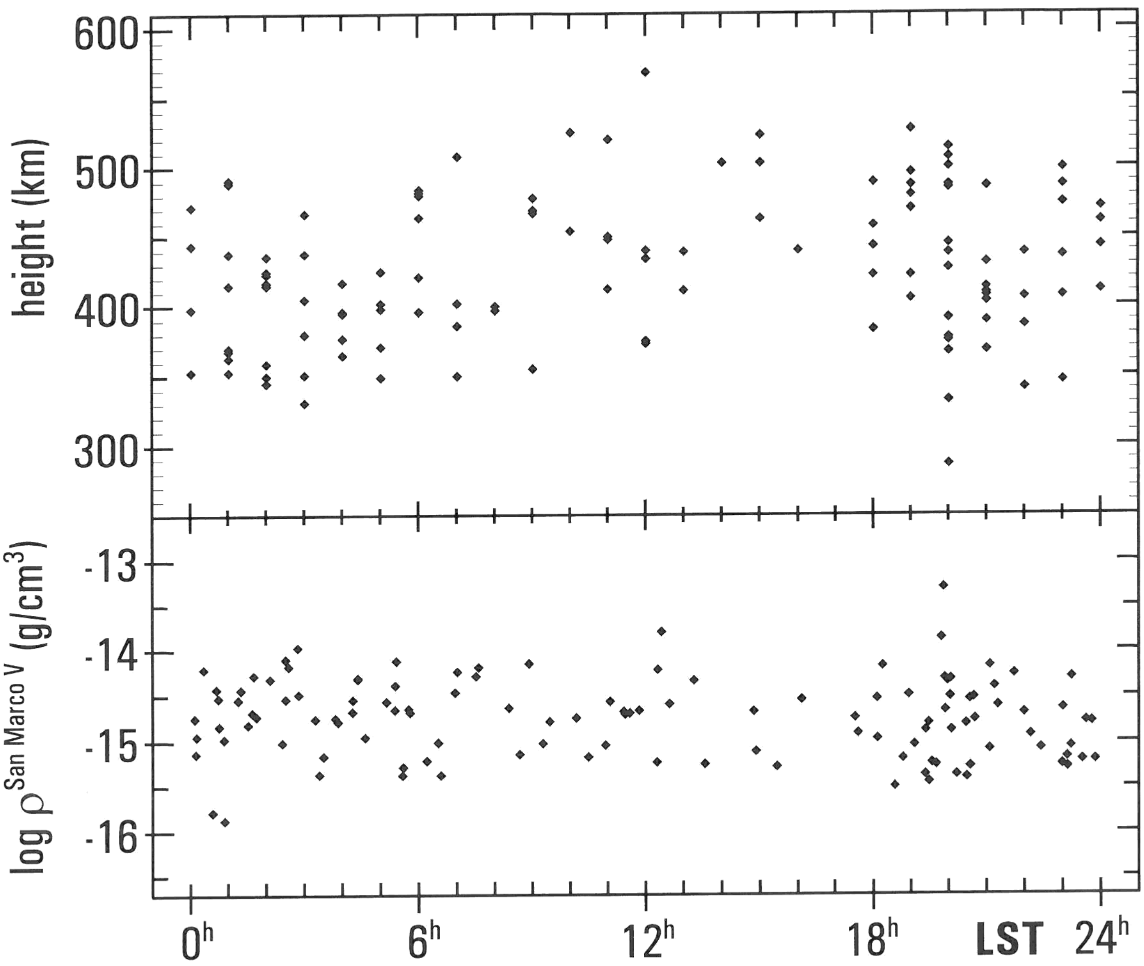
600
500
400
300
height (km)
-13
-14
-15
-16
log ρ San Marco V (g/cm3)
0h
6h
12h
18h
LST
24h

Fig. 10